A simulation study to compare ^{210}Pb dating data analyses

Marco A Aquino-López[*†] Nicole K. Sanderson[‡] Maarten Blaauw[§]
J Andrés Christen[¶]

Abstract

The increasing interest on understanding the impact that humans have in the environment, have lead to a considerable amount of studies which focus on sediment analysis in the last 200 years. Dating this period is often complicated by poor resolution and large errors associated with radiocarbon (14C) ages, which is the most popular dating technique. The use of lead-210 (^{210}Pb) is a popular method as it allows for the measurement of absolute and continuous dates for this period of time. ^{210}Pb dating method has traditionally relied on the Constant Rate of Supply (CRS) model which uses the radioactive decay equation resulting in a restrictive model to approximate dates.

Recent studies in radiocarbon age-depth models (Blaauw et al., 2018) have shown that the Bayesian age-depth models provide a more reliable and trustworthy chronology. With the recent development of *Plum* (Aquino-López et al., 2018), the only Bayesian alternative to ^{210}Pb dating, this work seeks to develop an objective comparison between the classical approach to ^{210}Pb dating (CRS) and its Bayesian alternative (*Plum*). The comparison was achieved by three different simulations which follow three different sedimentation processes and all three simulations follow the assumptions imposed by the CRS model, this to allow for a fair and honest comparison. The result of this study not only confirms the results obtained by Blaauw et al. (2018), but it also show a series of worrying outcomes regarding the accuracy and precision of the CRS model, mainly that the uncertainty associated to the model is always insufficient to capture the true values even when the sediment is entirely dated. The most concerning result is the fact that the CRS model does not appear to improve its accuracy as more information is available, which results in a model which accuracy is chaotic and unpredictable. On the other hand, the Bayesian alternative (*Plum*) provides consistently accurate results even with few samples, and its accuracy and precision constantly improve as more information is available.

Keywords: Plum, Age-depth models, Chronology, Constant Rate of Supply, Comparison.

[*]Centro de Investigación en Matemáticas (CIMAT), Jalisco s/n, Valenciana, 36023 Guanajuato, Gto, Mexico. email: aquino@cimat.mx

[†]Corresponding author.

[‡]College of Life and Environmental Sciences, University of Exeter, Exeter, EX4-4QJ, UK. email: N.K.Sanderson@exeter.ac.uk

[§]School of Natural and Built Environment, Queen's University Belfast, Belfast, BT7-1NN, UK. email:maarten.blaauw@qub.ac.uk

[¶]Centro de Investigación en Matemáticas (CIMAT), Jalisco s/n, Valenciana, 36023 Guanajuato, Gto, Mexico. email: jac@cimat.mx

1 Introduction

^{210}Pb is a radioactive nuclide which naturally forms in the atmosphere (as well as in sediments) as result of the decay chain of ^{238}U. This isotope, with a half-life if 22.23 yr, is commonly used to date recent recently accumulated sediments (< 150 to 200 yr). Unlike to other dating techniques such as ^{14}C (radiocarbon dating), a single measurement of ^{210}Pb is useless for dating and it is only when a suitable portion of the decay curve is measured (together with certain assumptions about the sedimentation process) that a chronology can be established. In recent decades, increasing amounts of palaeoecological and pollution studies have focused on recent sediments (e.g., Mustaphi et al., 2019) in order to measure the human impact in the environment. These studies strongly depend on the accuracy of the chronologies in order to correctly assign dates to chemical and biological changes. That is, unlike other dating techniques, an analysis of a series (data set) of ^{210}Pb measurements most be carried out in order to obtain meaningful dates. In a lake sediment, or any other, sedimentation process, samples are taken along a core at different depths, from which ^{210}Pb activity is measured. The whole series of ^{210}Pb measurements need to be analyzed to attempt to produce a coherent chronology, see Aquino-López et al. (2018).

A range of traditional data analyses, or so called "models", are available for dating recent sediment using ^{210}Pb, most notably are the Constant Rate of Supply (CRS), Constant Flux:Constant sedimentation (CF:CS) and Constant Initial Concentration (CIC) models (Appleby and Oldfield, 1978; Robbins, 1978; Sanchez-Cabeza and Ruiz-Fernández, 2012) . The CRS model, also known as Constant Flux - (CF) model is by far the most popular (see Figure 1) and has the most flexible assumptions. The CRS model assumes a constant supply of ^{210}Pb to the sediment from the atmosphere and allows for changes in the sedimentation rate. In order to estimate a chronology the CRS model uses a ratio between the complete "inventory" (the complete estimate of the radioactivity in the column of the sediment between the surface and a certain depth where ^{210}Pb from the atmosphere can no longer be found) and the remaining inventory from depth x ($t(x) = \frac{1}{\lambda} \log\left(\frac{A_0}{A_x}\right)$, where A_0 is the complete inventory, λ the decay constant of the ^{210}Pb $\approx .03114$).

Other, more restrictive models such as CF:CS and CIC requiere the assumption of a constant supply of ^{210}Pb as well as other assumptions of the sedimentation process. The flexibility of the CRS, regarding its assumptions, comes at the cost of the need to measure a sufficient portion of the inventory or the use of interpolation in order to properly estimate the complete inventory of ^{210}Pb in the sediment.

This model has received several revisions in order to improve its accuracy and applicability. There are two types of revisions to this model: revisions to its uncertainty (Binford, 1990; Appleby, 2001; Sanchez-Cabeza et al., 2014) and to its applicability when extra information is available, such as extra dating sources (e.g. ^{137}Cs dates) or laminated sediments (Appleby, 1998, 2001, 2008).

A recent inter-laboratory experiment (Barsanti et al., 2020), presented a series of ^{210}Pb data to different laboratories around the world. Each laboratory was ask to provide a chronology given the provided data. This experiment resulted in a whole range of different chronologies, given the same data, not only when

different models were used, but even when the same model was applied. The authors strongly advised to the use of independent time markers (extra dating sources) to validae of the chronologies. This research clearly shows the effect that user decisions have on the resulting chronologies. And indeed, this becomes extremely important when trying to replicate the resulting chronologies. Users trying to replicate these chronologies will not only need access to the raw data but also to every user decision which lead to the resulting chronology; unfortunately these raw data and decisions are rarely reported.

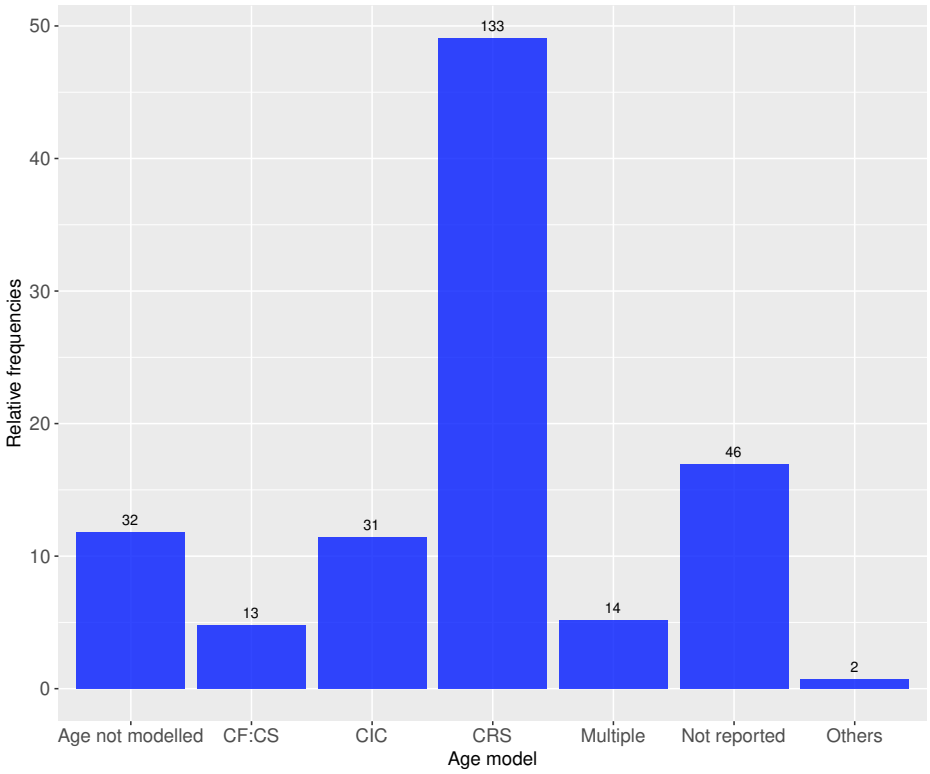

Figure 1: Frequency of ^{210}Pb dating models used in papers between 1964 and 2017. Data gathered by Mustaphi et al. (2019) from a literature review of 271 papers. The models include CF:CS model (The Constant Flux - Constant Sedimentation; Robbins, 1978), CIC (Constant Initial Concentration) (Goldberg, 1963; Crozaz et al., 1964; Robbins, 1978) and CRS - (Constant Rate of Supply; Appleby and Oldfield, 1978; Robbins, 1978).

Recently Aquino-López et al. (2018) presented an alternative to these classical models, by introducing *Plum* (a Bayesian approach to ^{210}Pb dating). This model treats every data point as originating from a system, which includes the sedimentation process as well as the decay process. It also incorporates an important variable to the inferred processes, namely, the levels of supported ^{210}Pb, which naturally forms in the sediment and is normally threaded as a hindrance variable. *Plum* assumes that there exists an (unknown) age-depth function $t(x)$ that relates depth x with calendar age $t(x)$. Conditional on $t(x)$, the following model

is assumed for measured ^{210}Pb y_i for the sediment section form depths $x_i - \delta$ to x_i

$$y_i \mid P_i^S, \Phi_i, \bar{t} \sim \mathcal{N}\left(A_i^S + \frac{\Phi_i}{\lambda}\left(e^{-\lambda t(x_i-\delta)} - e^{-\lambda t(x_i)}\right), (\sigma_i \rho_i)^2\right). \quad (1)$$

Here A_i^S is the supported ^{210}Pb in the sample and Φ_i the supply of ^{210}Pb to the sediment, see Aquino-López et al. (2018) for details. The age-depth model $t(x)$ is based on a piece-wise linear model constrained by prior information on the sediment's accumulation rates (Blaauw and Christen, 2011).

This treatment of the data allows for a formal statistical inference and by using a Bayesian approach all the parameters of the model can be inferred. This differs from the CRS model because the latter uses the decay equation to obtained the age-depth function (which results in a more restrictive age-depth model), removes assumed values of supported ^{210}Pb before modelling, and does not provide a formal statistical inference. *Plum* has shown to provide accurate results with a realistic precision depending on the different case scenarios (Aquino-López et al., 2020) - both in simulations as well as for real cores. Under optimal conditions *Plum* and the CRS model have shown to provide similar results (Aquino-López et al., 2020) with *Plum* providing more realistic uncertainties, with minimal user interaction.

Blaauw et al. (2018) presented a comparison between classical and Bayesian age-depth models construction, both for real and simulated ^{14}C-dated cores. They concluded that Bayesian age-depth models provide a more accurate result and more realistic uncertainties under a wide range of scenarios. In this study, we compare the CRS model (by far the most popular age-depth model for ^{210}Pb) against *Plum* using simulated cores, i.e. sedimentation "scenarios". The objective of this study is to observe if the results that Blaauw et al. (2018) obtained are maintained in a more difficult situation as that of the construction of age-depth models using ^{210}Pb. We also wish to observe the learning process of each of the models and how much information is needed to obtained a reasonable chronology given a particular model.

The paper is organized as follows: first section sets the tools for the comparison, it describes the simulations of the three different scenarios and we described a parameter which will facilitate the comparison called information percentage. Section 3 describes the comparison for both the overall chronologies and by single depths. Lastly section 4 presents the conclusions and discussion of the results obtained in section 3.

2 Simulated data

In order to observe the accuracy and precision of any model, we need data where the true age-depth function is known. Blaauw et al. (2018) presented a methodology for simulating radiocarbon dates and their uncertainty, whereas Aquino-López et al. (2018) presented an approach for simulating ^{210}Pb data given an age-depth function $t(x)$. It is important to note that these simulations follow the equations presented by Appleby and Oldfield (1978); Robbins (1978) guaranteeing that the CRS assumptions are met. By using the approach presented by Aquino-López et al. (2018) for simulating ^{210}Pb data and the structure of uncertainty estimation presented by Blaauw et al. (2018), reliable ^{210}Pb simulated data can be obtained.

2.1 Simulation Construction

Three different scenarios (see table 2.1) were chosen for our simulations of sedimentation, each with their own age-depth functions and parameters. This scenarios were selected as they provide three challenges for the models: the first scenario presents an age-depth function which is quite common for recent sediments (with less compaction toward the surface at 0 cm depth), the second scenario presents a challenging core as the function replicates a drastic and quick change in sediment behaviour around depth 15 cm depth, and lastly proposal three presents a cyclic and periodic change in accumulation. Using the age-depth functions and defined parameters in table 2.1, we may obtained the ^{210}Pb activity at any depth or interval. These concentrations may be interpreted as error-free measurements, see Figure 2 . Because ^{210}Pb activity measurement is subject to error, we need to replicate the measurement errors. Blaauw et al. (2018) presents error structure for radiocarbon dates. We can use this structure to our ^{210}Pb measurements as both measurements are subject to similar measurement problems.

Label	Age-depth function $t(x)$	Φ $(\frac{Bq}{m^2 yr})$	Supported ^{210}Pb $(\frac{Bq}{kg})$
Scenario 1	$\frac{x^2}{4} + \frac{x}{2}$	100	10
Scenario 2	$12x - .2x^2$	50	25
Scenario 3	$8x + 25\sin(\frac{x}{\pi})$	500	15

Table 1: Simulated age-depth function and parameters used in each scenario

Let $C_{\hat{x}}$ be the true ^{210}Pb concentration in the interval $\hat{x} = [x-\delta, x)$, given the age-depth function $t(x)$ and parameters Φ and A^S in each scenario. To simulate disturbances in the material, we can introduce scatter centred around the true value, $\theta \sim \mathcal{N}\left(C_{\hat{x}}, y_{scat}^2\right)$, where x_{scat}^2 is the amount of scatter for this variable (in this case $y_{scat}^2 = 10$). Now, to replicate outliers, a shift from the true value (x_{shift}) is defined, which occurs with a probability p_{out}. This results in a new variable θ' which is defined as

$$\theta' = \begin{cases} \mathcal{U}(\theta - x_{shift}, \theta + x_{shift}), & p_{out} \\ \theta, & 1 - p_{out} \end{cases}. \tag{2}$$

Finally, to simulate the uncertainty provided by the laboratory, we can define the simulated measurements as $y(\theta') \sim \mathcal{N}\left(\theta', \sigma_R^2\right)$, where σ_R is the standard deviation reported by the laboratory. σ_R is defined as $\sigma_R = \max\left(\sigma_{min}, \mu(\theta')\ \varepsilon\ y_{scat}\ \right)$, where σ_{min} is the minimum standard deviation assigned to a measurement. This variable differs between laboratories (we will be using a default value of 1 Bq/kg). Finally, ε is the analytical uncertainty (default .01) and y_{scat} an error multiplier (default 1.5). The default parameters were set in accordance with Blaauw et al. (2018). For this this study we created a data set for each simulation by integrating in intervals of δ =1 cm, for depths from 0 to 30 cm where equilibrium was guaranteed (Aquino-López et al., 2018). The complete simulated ^{210}Pb data sets can be found in the Supplementary Material

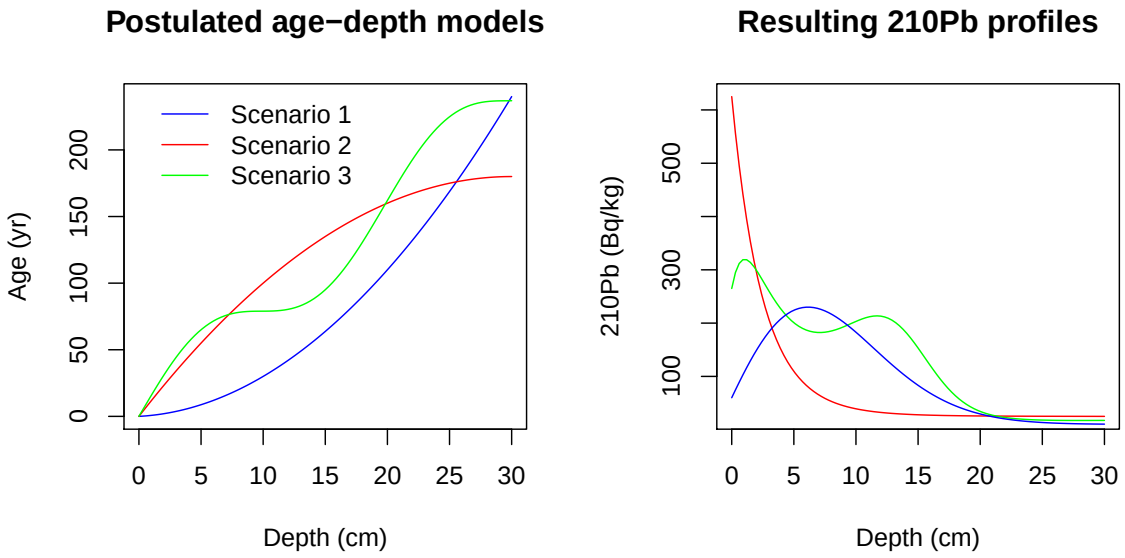

Figure 2: Simulated sedimentation scenarios with their corresponding ^{210}Pb profiles. Right: Age-depth function for the three different scenarios (Table 2.1). Left: Corresponding ^{210}Pb activity profiles in relation to depth.

5.

3 Model Comparison

To allow for a reasonable comparison between models and to observe the effect that different percentage of information have on the accuracy and precision of ^{210}Pb models, we used the three simulated data sets created in the previous section. These simulated cores were randomly selected given a percentage of information (e.g. for a 20% information sample, in a 30 cm cores, 6 random 1-cm samples were selected). Because the CRS model assumes that background activity has being reached (in order to reduce user manipulation), we decided to fix the last sample (30 cm depth) for every case. This guaranties the proper use of the CRS model and also gives the model a single last depth to be removed as it is common practice when using the CRS model. 100 different samples were randomly selected for information percentages from 10% to 95% at 5% intervals (i.e., 10%, 15%, 20%,...,95%) and the complete sample was also used (i.e 100% percentage of information sample). After a random sample was selected, both the CRS model and *Plum* were applied to the data set. To have an objective comparison, both models were run with their default configuration (*Plum* with default settings and CRS estimates and uncertainties as described in Appleby (2001)) and then their outputs compared against the true age value.

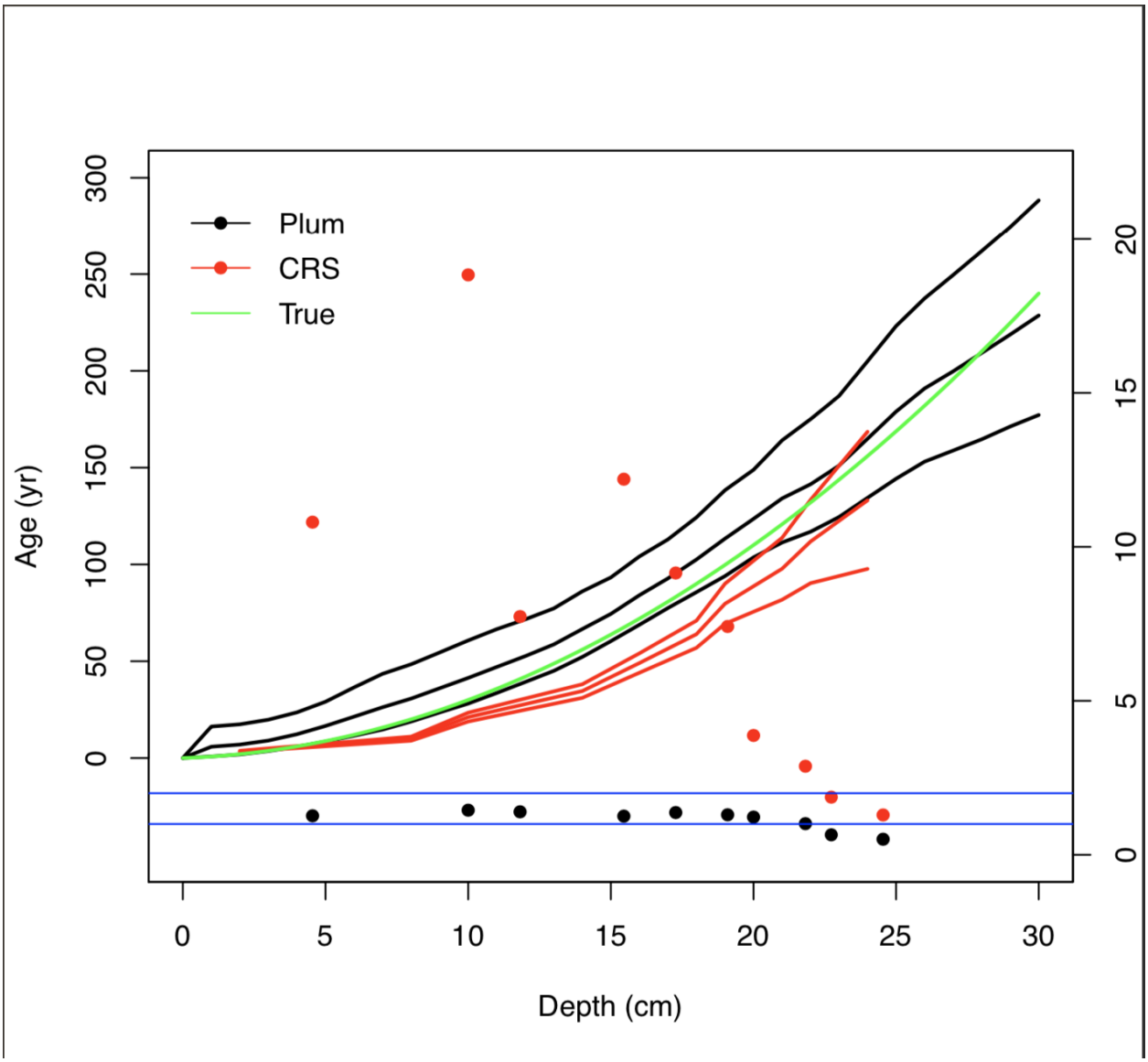

Figure 3: Comparison between *Plum* and the CRS model against the true age-depth model using 50% of the information percentage (using 1-cm samples at depths 2, 8, 10, 14, 16, 18, 19, 21, 22, 24, 25, 27, 28, 29, 30). Lines show the age estimates with the 95% credible intervals (*Plum*) and the 95% confidence interval (CRS). Dots show the normalized offset, distance between the inferred age and the true age in relation to the standard error (the standard deviation in the case of the CRS and the length of the confidence interval divided by 4 in the case of *Plum*).

Figure 3 shows an example of the comparison between the ^{210}Pb models against the true value. Because we are dealing with 5333 simulations, in order to observe the precision and accuracy in general, we decided to calculate the mean offset to the true age-depth model (in yr), the mean of length of the 95% intervals (in yr), as well as the mean normalized accuracy (this indicates how far the model is from the true value given its own uncertainty at that depth).

Figure 4 show similar results those presented by Blaauw et al. (2018). The classical model (CRS) at first appears to provide a similar results (similar offsets) to the Bayesian alternative (*Plum*), but at higher estimated precision (if we only look at the length of the 95% interval). These results can be misleading if we do not analyze the effects of both the offset and length of the interval together. To have a more realistic representation of how the models capture the true age-depth models we can observe the normalized offset. This variable shows to which degree the average models contain the truth within their uncertainty intervals (normalized to one standard deviation). Any model with normalized offset larger than two (two standard deviations) is incapable of capturing the true ages within their uncertainty intervals. This means that the CRS estimates smaller uncertainties, yet at the cost of its accuracy. It also appears that the length of the 95% interval and offset are not affected by how much information is provided to the CRS model.

On the other hand, *Plum* shows more accurate results as more information is given to the model. This again coincides with the results found by Blaauw et al. (2018). When we observe the regular offset (not normalized), we observed that textitPlum provides a smaller offset in comparison to the CRS model; this in combination with slightly larger modelled uncertainties results in consistently accurate age-depth models which are capable of capturing the true values within their uncertainty intervals. This result supports the claim that *Plum* provides more realistic uncertainties than those of the CRS.

Another important statistic to take into account is that 87.86% (4686/5333) of *Plum*'s runs remain under the 2 standard deviations, whereas the CRS model only has 7.48% (399/5333) under the 2 standard deviations, and only 0.54% (29/5333) lies under the 1 standard deviation, which is the most commonly reported interval when reporting CRS results. We can also observe a clear structure in the way *Plum* increases its accuracy and precision to obtained a better chronology as more information is available, whereas the CRS model does not appears to learn from more data. These results are presented for the overall chronology (the mean offset, interval and normalized offset of the overall chronology). In order to observe if certain models are better predicting at certain section of the sediment, we have to look at the normalized offset of every depth.

Figure 5 shows the normalized accuracy of every simulation by depth for both models. *Plum* shows a clear learning structure which depends on the information available to the model. The information percentage appears to be irrelevant to the accuracy of the CRS model, contrary to the results obtained by *Plum*. It is important to note that the inaccuracies of the CRS model are not exclusive to any particular sections of the chronology; this is most likely caused by the small uncertainties estimated by the CRS model.See below for a discussion of how *Plum* behaved in sedimentation simulation 2.

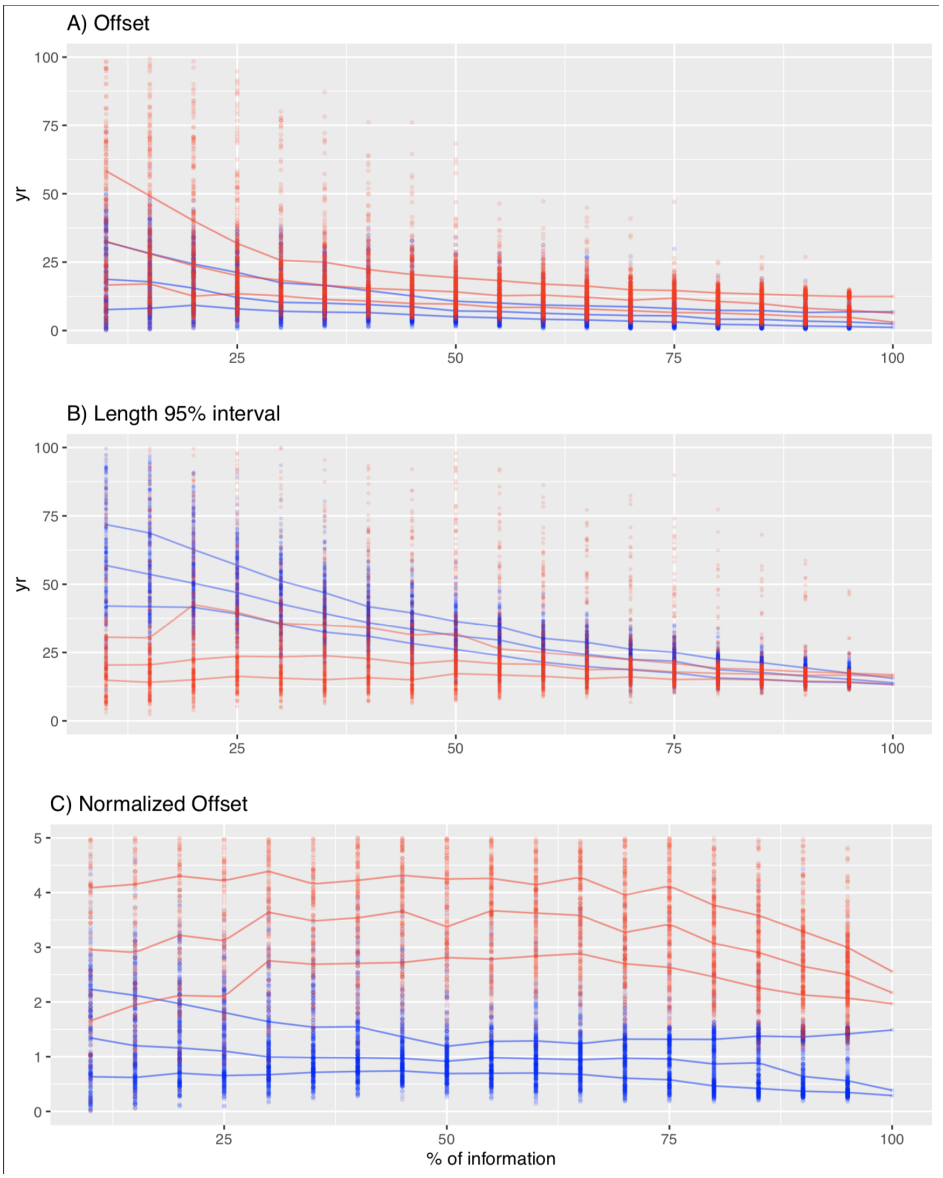

Figure 4: Top panel A) shows the offset between the modelled and true age of the CRS (red) and *Plum* (blue). This panel shows how *Plum* provides a small offset in almost every scenario with both models improving their offset as more information is available. Middle panel B) shows the 95% confidence intervals. It is clear, from this panel, than the uncertainty provided by *Plum* is a lot bigger for low percentage of information and it constantly improves as more data is available, whereas the length of the intervals provided by the CRS appear to stay constant regardless of the available information. Bottom panel C) shows the normalized offsets, presenting the distance between the modelled age and the true age normalized divided by the standard deviation (in the case of *Plum*, the length of the 95% interval divided by 4). This panel presents a worrying situation where the CRS model's calculated standard deviation (on average) is incapable of of capturing the true age. On the other hand, *Plum*'s credible intervals almost always capture the true age even when little information is available.

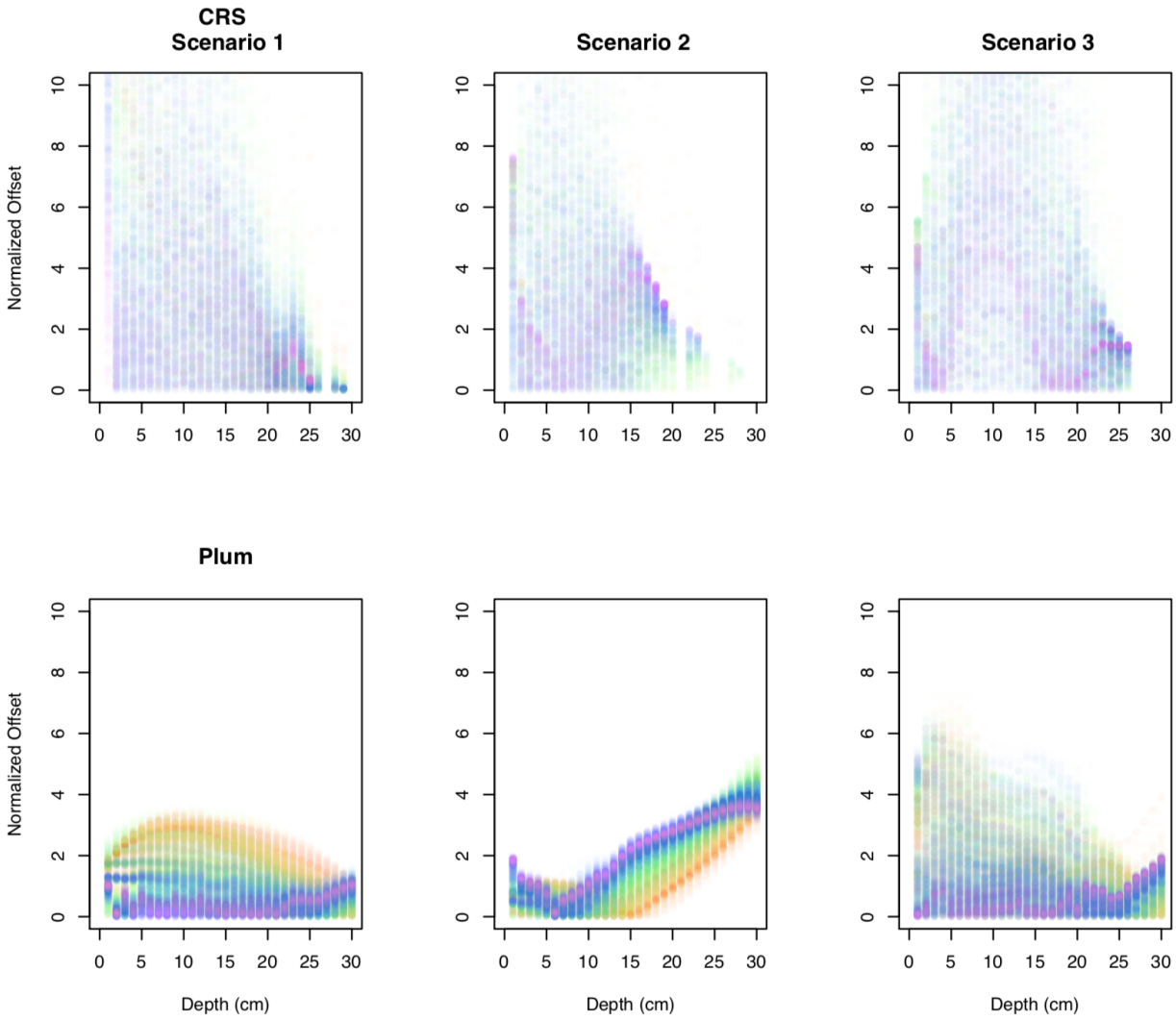

Figure 5: Normalized offset of every sampling sample at every depth for the three simulated scenarios - CRS age estimates at samples depths and *Plum*'s age estimates at 1 cm intervals. Dots go from lowest information percentage samples (few dated depths; red) to high percentage samples (nearly completely dated cores; purple). The CRS's normalized offset shows no structure at any particular depth regardless of the available information. This means that the model can provide a reasonable chronology with low levels of information or a very inaccurate age estimate with high levels of information at any given depth resulting in a distrustful age-depth model. On the other hand, *Plum* demostrares a systematic improvement in its age estimates as more data is available. This results assures that a Bayesian approach would consistently provide more reliable results.

4 Conclusions and Discussion

These results clearly show the bias of the CRS model. Aquino-López et al. (2018) discussed this point and states that the bias is the product of the use of a logarithmic function for the age-depth function. It is also evident from these results that the CRS model's uncertainty estimates are not sufficient to capture the true age-depth function. This is an important point given the fact that it is common practice among the ^{210}Pb dating community to report credible intervals to one single deviation (instead of the 95% confidence intervals, which have become common practice in most other chronology reconstructions). Other confidence intervals can be calculated for this model (Sanchez-Cabeza et al., 2014) but the fact that these intervals are even smaller than the ones obtained by error propagation (Appleby, 2001) is of concern.

Previous work on model comparison (Barsanti et al., 2020) has shown the problems with the variability of ^{210}Pb results even when different users apply the same or similar models to a single set of data. In this work, user input was reduced to the minimum in an effort to show the potential effects of different information percentages have on the resulting chronology. The results of this experiment showed that the CRS model can provide extremely different results even when the data originates from the same data set. Figure 4 showed that the CRS model appears not to learn from using more data. This explains why over the years, many authors have insisted in the use of other dating techniques to validate the chronology provided by the CRS model (Sanchez-Cabeza and Ruiz-Fernández, 2012; Barsanti et al., 2020; Aquino-López et al., 2020). These results highly encourage the need of validating the CRS chronology before it is use.

On the other hand, *Plum* shows a consistently accurate result by capturing the true values within the 95% credible intervals in by most of the simulated sampling strategies. It is important to note that one of the big advantages of *Plum* is its increasing accuracy and precision reduction as more data becomes available. In the case of proposal 2, we observe that *Plum* appears to behaves worse as more data is available, which would be of concern if we do not take into consideration that this sedimentation simulation was extremely unusual in the real world and also if users would not double check the resulting chronologies. If more information is available about the core or the sediment, this information can easily be implemented as prior information in *Plum*, and this will result in a much better chronology. It is also important to note that even when *Plum* performs badly in this specific case, it is providing a much better chronology to upper first 10-15 cm of the core than that of the chaotic CRS age-depth model model.

In conclusion, the use of CRS can only be accommodated if users may validate their chronology with external dates as the ^{137}Cs time markers or other time markers. If not extra information is available for this validation, the use of *Plum* is still valid, specially if provide it with as as many ^{210}Pb measurements as possible (at least 60% of the available information of the core). Even so, additional dating information may also be formally included in *Plum* to improve the resulting chronology (Aquino-López et al., 2018, 2020).

References

Appleby, P. (2008). Three decades of dating recent sediments by fallout radionuclides: a review. *The Holocene*, 18(1):83–93.

Appleby, P. and Oldfield, F. (1978). The calculation of lead-210 dates assuming a constant rate of supply of unsupported 210pb to the sediment. *Catena*, 5(1):1–8.

Appleby, P. G. (1998). Dating recent sediments by Pb-210: Problems and solutions. *Proc. 2nd NKS/EKO-1 Seminar, Helsinki, 2-4 April 1997, STUK, Helsinki*, pages 7–24.

Appleby, P. G. (2001). Chronostratigraphic techniques in recent sediments. *Tracking Environmental Change Using Lake Sediments: Basin Analysis, Coring, and Chronological Techniques*, pages "171–203".

Aquino-López, M. A., Blaauw, M., Christen, J. A., and Sanderson, N. K. (2018). Bayesian analysis of 210pb dating. *Journal of Agricultural, Biological and Environmental Statistics*, 23(3):317–333.

Aquino-López, M. A., Ruiz-Fernández, A. C., Blaauw, M., and Sanchez-Cabeza, J.-A. (2020). Comparing classical and bayesian 210pb dating models in human-impacted aquatic environments. *Quaternary Geochronology*, 60:101106.

Barsanti, M., Garcia-Tenorio, R., Schirone, A., Rozmaric, M., Ruiz-Fernández, A., Sanchez-Cabeza, J., Delbono, I., Conte, F., Godoy, J. D. O., Heijnis, H., Eriksson, M., Hatje, V., Laissaoui, A., Nguyen, H., Okuku, E., Al-Rousan, S. A., Uddin, S., Yii, M., and Osvath, I. (2020). Challenges and limitations of the 210pb sediment dating method: Results from an IAEA modelling interlaboratory comparison exercise. *Quaternary Geochronology*, 59:101093.

Binford, M. W. (1990). Calculation and uncertainty analysis of ^{210}Pb dates for PIRLA project lake sediment cores. *Journal of Paleolimnology*, 3:253–267.

Blaauw, M. and Christen, J. A. (2011). Flexible paleoclimate age-depth models using an autoregressive gamma process. *Bayesian Analysis*, 6(3):457–474.

Blaauw, M., Christen, J. A., Bennett, K., and Reimer, P. J. (2018). Double the dates and go for Bayes — impacts of model choice, dating density and quality on chronologies. *Quaternary Science Reviews*, 188:58–66.

Crozaz, G., Picciotto, E., and de Breuck, W. (1964). Antarctic snow chronology with pb210. *Journal of Geophysical Research*, 69(12):2597–2604.

Goldberg, E. D. (1963). Geochronology with pb-210. *Radioactive Dating*, pages 121–131.

Mustaphi, C. J. C., Brahney, J., Aquino-López, M. A., Goring, S., Orton, K., Noronha, A., Czaplewski, J., Asena, Q., Paton, S., and Brushworth, J. P. (2019). Guidelines for reporting and archiving 210pb sediment chronologies to improve fidelity and extend data lifecycle. *Quaternary Geochronology*, 52:77–87.

Robbins, J. (1978). Geochemical and geophysical applications of radioactive lead. *The biogeochemistry of lead in the environment*, pages 285–393.

Sanchez-Cabeza, J. A. and Ruiz-Fernández, A. C. (2012). 210Pb sediment radiochronology: An integrated formulation and classification of dating models. *Geochimica et Cosmochimica Acta*, 82:183–200.

Sanchez-Cabeza, J. A., Ruiz-Fernández, A. C., Ontiveros-Cuadras, J. F., Pérez Bernal, L. H., and Olid, C. (2014). Monte Carlo uncertainty calculation of 210Pb chronologies and accumulation rates of sediments and peat bogs. *Quaternary Geochronology*, 23:80–93.

5 Supplementary Material

Data for each simulation and code used is hosted at: https://github.com/maquinolopez/Paper_Simulations

Label	Depth (cm)	Density (g/cm^3)	210Pb (Bq/kg)	sd(210Pb)	Thickness (cm)	226Ra (Bq/kg)	sd(226Ra)
Sim01-01	1	0.10009	63.50103	2.85755	1	23.8045	1.125
Sim01-02	2	0.10064	80.08738	3.60393	1	23.2924	1.125
Sim01-03	3	0.10173	98.32806	4.42476	1	23.434	1.125
Sim01-04	4	0.10334	125.45705	5.64557	1	26.0873	1.125
Sim01-05	5	0.10547	141.27971	6.35759	1	22.8041	1.125
Sim01-06	6	0.10809	130.27571	5.86241	1	23.4333	1.125
Sim01-07	7	0.11116	134.04051	6.03182	1	25.6156	1.125
Sim01-08	8	0.11466	129.69245	5.83616	1	26.1371	1.125
Sim01-09	9	0.11855	134.93655	6.07214	1	25.4813	1.125
Sim01-10	10	0.12278	109.39886	4.92295	1	25.8877	1.125
Sim01-11	11	0.12731	110.68133	4.98066	1	24.4414	1.125
Sim01-12	12	0.13209	102.38094	4.60714	1	24.9053	1.125
Sim01-13	13	0.13706	75.80895	3.4114	1	22.9151	1.125
Sim01-14	14	0.14218	77.60406	3.49218	1	24.4808	1.125
Sim01-15	15	0.14738	68.4401	3.0798	1	24.9343	1.125
Sim01-16	16	0.15262	60.72037	2.73242	1	25.2659	1.125
Sim01-17	17	0.15782	50.28147	2.26267	1	22.961	1.125
Sim01-18	18	0.16294	44.24641	1.99109	1	22.9139	1.125
Sim01-19	19	0.16791	39.85997	1.7937	1	28.3774	1.125
Sim01-20	20	0.17269	38.40823	1.72837	1	23.5379	1.125
Sim01-21	21	0.17722	32.75922	1.47416	1	25.4363	1.125
Sim01-22	22	0.18145	28.02545	1.26115	1	24.8995	1.125
Sim01-23	23	0.18534	27.8749	1.25437	1	22.6783	1.125
Sim01-24	24	0.18884	30.74797	1.38366	1	24.8575	1.125
Sim01-25	25	0.19191	28.36187	1.27628	1	24.8724	1.125
Sim01-26	26	0.19453	27.24535	1.22604	1	24.3778	1.125
Sim01-27	27	0.19666	23.59236	1.06166	1	24.7209	1.125
Sim01-28	28	0.19827	25.74855	1.15868	1	24.6615	1.125
Sim01-29	29	0.19936	25.05368	1.12742	1	24.7199	1.125
Sim01-30	30	0.19991	25.0065	1.12529	1	24.4937	1.125

Label	Depth (cm)	Density (g/cm^3)	210Pb (Bq/kg)	sd(210Pb)	Thickness (cm)	226Ra (Bq/kg)	sd(226Ra)
Sim02-01	1	0.1001	909.3928	40.9227	1	8.9761	0.45
Sim02-02	2	0.1006	683.9989	30.7799	1	10.0607	0.45
Sim02-03	3	0.1017	453.0503	20.3873	1	9.8701	0.45
Sim02-04	4	0.1033	310.7897	13.9855	1	10.37	0.45
Sim02-05	5	0.1055	218.0058	9.8103	1	10.0418	0.45
Sim02-06	6	0.1081	158.6974	7.1414	1	10.104	0.45
Sim02-07	7	0.1112	113.9062	5.1258	1	10.2049	0.45
Sim02-08	8	0.1147	75.5493	3.3997	1	9.334	0.45
Sim02-09	9	0.1185	56.6252	2.5481	1	10.5145	0.45
Sim02-10	10	0.1228	44.1595	1.9872	1	9.8677	0.45
Sim02-11	11	0.1273	34.7448	1.5635	1	9.7694	0.45
Sim02-12	12	0.1321	25.384	1.1423	1	10.5134	0.45
Sim02-13	13	0.1371	24.0007	1.08	1	10.4589	0.45
Sim02-14	14	0.1422	21.3643	1	1	9.9504	0.45
Sim02-15	15	0.1474	17.7932	1	1	10.5135	0.45
Sim02-16	16	0.1526	15.0416	1	1	10.3362	0.45
Sim02-17	17	0.1578	14.2937	1	1	10.5131	0.45
Sim02-18	18	0.1629	12.3844	1	1	10.368	0.45
Sim02-19	19	0.1679	12.6023	1	1	10.5297	0.45
Sim02-20	20	0.1727	11.9329	1	1	10.0924	0.45
Sim02-21	21	0.1772	9.301	1	1	10.118	0.45
Sim02-22	22	0.1815	10.7777	1	1	10.249	0.45
Sim02-23	23	0.1853	12.9491	1	1	10.134	0.45
Sim02-24	24	0.1888	10.6571	1	1	10.1151	0.45
Sim02-25	25	0.1919	9.6297	1	1	9.6608	0.45
Sim02-26	26	0.1945	8.4331	1	1	8.7821	0.45
Sim02-27	27	0.1967	10.4921	1	1	9.8995	0.45
Sim02-28	28	0.1983	11.135	1	1	9.2481	0.45
Sim02-29	29	0.1994	10.109	1	1	10.4398	0.45
Sim02-30	30	0.1999	9.5404	1	1	10.1114	0.45

Label	Depth (cm)	Density (g/cm^3)	210Pb (Bq/kg)	sd(210Pb)	Thickness (cm)	226Ra (Bq/kg)	sd(226Ra)
Sim03-01	1	0.1001	6384.1354	287.2861	1	15.8007	0.675
Sim03-02	2	0.1006	3550.0809	159.7536	1	14.5245	0.675
Sim03-03	3	0.1017	1954.5702	87.9557	1	15.6527	0.675
Sim03-04	4	0.1033	1183.8917	53.2751	1	14.5175	0.675
Sim03-05	5	0.1055	760.2132	34.2096	1	14.9242	0.675
Sim03-06	6	0.1081	360.2553	16.2115	1	14.801	0.675
Sim03-07	7	0.1112	212.9402	9.5823	1	14.8738	0.675
Sim03-08	8	0.1147	104.2684	4.6921	1	14.9028	0.675
Sim03-09	9	0.1185	44.3849	1.9973	1	15.0768	0.675
Sim03-10	10	0.1228	18.6447	1	1	15.3764	0.675
Sim03-11	11	0.1273	23.2778	1.0475	1	14.6231	0.675
Sim03-12	12	0.1321	53.1587	2.3921	1	15.1629	0.675
Sim03-13	13	0.1371	97.363	4.3813	1	14.3047	0.675
Sim03-14	14	0.1422	116.9788	5.264	1	14.0261	0.675
Sim03-15	15	0.1474	153.2901	6.8981	1	15.9723	0.675
Sim03-16	16	0.1526	151.8496	6.8332	1	14.7579	0.675
Sim03-17	17	0.1578	136.3609	6.1362	1	16.114	0.675
Sim03-18	18	0.1629	107.2736	4.8273	1	15.4595	0.675
Sim03-19	19	0.1679	76.8966	3.4603	1	15.9439	0.675
Sim03-20	20	0.1727	48.9213	2.2015	1	14.6235	0.675
Sim03-21	21	0.1772	40.4439	1.82	1	14.6716	0.675
Sim03-22	22	0.1815	26.5638	1.1954	1	16.2541	0.675
Sim03-23	23	0.1853	21.714	1	1	14.4826	0.675
Sim03-24	24	0.1888	17.6428	1	1	15.5109	0.675
Sim03-25	25	0.1919	17.3533	1	1	13.6898	0.675
Sim03-26	26	0.1945	17.4211	1	1	14.4684	0.675
Sim03-27	27	0.1967	16.4246	1	1	15.3889	0.675
Sim03-28	28	0.1983	12.4828	1	1	15.0698	0.675
Sim03-29	29	0.1994	13.5514	1	1	15.2346	0.675
Sim03-30	30	0.1999	14.3145	1	1	14.7846	0.675